

The Crystallization Behavior and Mechanical Properties of Polylactic Acid in the Presence of a Crystal Nucleating Agent

Zhaobin Tang, Chuanzhi Zhang, Xiaoqing Liu, Jin Zhu

Ningbo Key Laboratory of Polymer Materials, Ningbo Institute of Material Technology and Engineering, Chinese Academy of Sciences, Ningbo, Zhejiang 315201, People's Republic of China

Received 14 January 2011; accepted 25 April 2011

DOI 10.1002/app.34799

Published online 31 December 2011 in Wiley Online Library (wileyonlinelibrary.com).

ABSTRACT: The crystallization behavior of polylactic acid (PLA) was studied in the presence of a crystal nucleating agent, ethylenebis(hydroxystearamide) (EBH). The crystallization rate and crystallinity were significantly increased with addition of EBH. The isothermal crystallization half-time at 105°C was decreased from 18.8 minutes for neat PLA to 2.8 minutes for PLA with 1.0 wt % of EBH. The crystallinity of PLA with 1.0 wt % EBH was about 35% after 5-minute annealing at 105°C. Like neat PLA, the double melting peaks were also observed for nucleated PLA. The changes of the double melt peaks were investigated with various crystallization temperatures, heating rates, and

annealing times. The heat deflection temperature (HDT) of nucleated PLA was up to 93°C after annealing. The correlation between crystallinity and HDT was demonstrated. A percolation threshold of crystallinity was found corresponding to HDT. The crystal size of nucleated PLA was significantly decreased with addition of EBH. The mechanical properties of annealed PLA blends simultaneously showed improved modulus and impact strength. © 2011 Wiley Periodicals, Inc. *J Appl Polym Sci* 125: 1108–1115, 2012

Key words: polylactic acid; crystallization; nucleating agent; double melting; heat deflection temperature

INTRODUCTION

In recent years, much more attention has been directed to the aliphatic polyesters, which have been regarded as one of the most competitive biodegradable materials in the future^{1,2} because of the global concern on the “white pollution” caused by more and more nonbiodegradable polymers. Polylactic acid (PLA) as an aliphatic polyester thermoplastic with high strength and stiffness was especially investigated for a great number of commodity applications from a viewpoint of an environmentally degradable polymer and sustainable biomass resources.^{3,4}

However, PLA has many drawbacks, such as a poor gas barrier, low impact strength, low heat deflection temperature (HDT), and brittleness. In particular, the low HDT limits the applications of PLA. For example, the molded PLA parts could be deformed during transportation because the temperature at storing cabin was higher than HDT of PLA. Improvements in HDT must be done prior to wide applications. There are several methods to improve

HDT of PLA. Although the HDT of PLA could be improved through addition of inorganic fillers,^{5–7} the filler was not preferred concerning biodegradability of materials.⁸ Addition of nucleating agents into semi-crystalline polymer not only decreased the crystallization time,^{9–15} but also increased the mechanical properties.¹⁶ Since only a small amount of nucleating agent was needed, the biodegradability of PLA was not affected. Thus, understanding of the crystallization behavior of PLA in the presence of a nucleating agent would be helpful to make a heat resistant PLA.

The characterization of polymer melting and crystallization behavior has been performed with various experimental techniques.^{17–22} Many researchers have studied the crystallization behavior of the neat PLA under an isothermal crystallization condition.^{23–26} Yasuniwa et al.²⁷ reported the double melting behavior of PLA during heating scan of differential scanning calorimetry (DSC). Although the crystallization behavior of the PLA has been studied thoroughly, the crystallization behavior of the PLA in the presence of a physical nucleating agent has rarely been studied in detail. In this article, we will report our study on the crystallization behavior, physical properties, and morphology of PLA with a nucleating agent, ethylenebis(hydroxystearamide) (EBH). Meanwhile, the correlation of HDT and crystallinity will also be investigated.

Correspondence to: J. Zhu (jzhu@nimte.ac.cn).

Contract grant sponsor: Ningbo Key Lab of Polymer Science; contract grant number: 0802051041

EXPERIMENTAL

Raw materials

NatureWorks PLA 2002D (containing 1.5–2.0% of D isomer, $\overline{M}_n = 127,000$) was purchased from NatureWorks LLC (Minnetonka, MN). EBH was purchased from Weike Chemical, Jiujiang, China. All raw materials were dried at 85°C for 5 h under vacuum to remove moisture prior to processing.

Sample preparation

The blends in this study were prepared by melt extrusion. The PLA and EBH were firstly mixed together and then melt extruded using a Brabender twin screw extruder. The weight ratio of PLA and EBH was kept at 99/1. The extruder barrel was operated at the temperature of 185–190°C and a screw speed of 50 rpm. The dry mixture was starve-fed into the extruder from a K-Tron feeder operating at 30°C and screw speed of 50 rpm. The extruded pellets were dried at 85°C for 5 h and stored for further use.

Apparatus

Thermal properties

DSC (Mettler Toledo DSC) was used to determine degree of crystallinity (X_c), melt temperature (T_m), cold crystallization temperature (T_{c1}), and glass transition temperature (T_g). For isothermal melt crystallizations, the samples were first heated at 10°C/min to 200°C, held there for 3 min, and finally cooled at 50°C/min to 105°C at which the samples were held for isothermal melt crystallization. Immediately after the isothermal melt crystallization, the samples were cooled at 50°C/min to 25°C, and this was followed by heating at different heating rate to 200°C to examine their isothermal melt-crystallization behaviors. For nonisothermal melt crystallization, the samples were heated from 25 to 200°C at heating rate of 10°C/min, held for 3 min, and then quickly cooled to 25°C at cooling rate of 50°C/min. The heating curves were recorded by immediate heating of the cooled samples to 200°C at heating rate of 10°C/min. From these heating curves, T_g , T_{c1} , and the endothermic melting temperature (T_m) were obtained. The melt crystallization temperature (T_{c2}) was determined during the second cooling scan. The following equation was used to calculate the degree of crystallinity within the samples:

$$\% \text{Crystallinity} = X_c = 100 \times \frac{\Delta H_m - \Delta H_c}{\Delta H_m^\infty} \quad (1)$$

where ΔH_m is the measured endothermic enthalpy of melting and ΔH_c is the cold crystallization exothermic enthalpy during the heating scans. The theoretical melting enthalpy of 100% crystalline PLA was taken to be $\Delta H_m^\infty = 93.6$ J/g. The DSC was calibrated periodically with indium standards.

Wide-angle X-ray scattering

Samples taken directly out of DSC pans after the nonisothermal melt crystallization treatments were examined in the wide-angle X-ray diffraction (WAXD) system so that the thermal history of the X-ray samples was precisely known. WAXD (D8 Advance, Bruker AXS, Germany) patterns were obtained at room temperature (ca. 20°C) with a WAXD measurement system reported elsewhere.²⁸ Monochromatized Cu K α radiation ($\lambda = 1.542$ Å) was used as an incident X-ray beam. The diffracted X-ray intensity was detected with a position sensitive proportional counter (PSPC) system. The diffraction angles reported for α -aluminum oxide (α -Al₂O₃) were used as a standard.

Optical microscopy

Optical microscopy was then carried out under polarized light to observe the formation and size of the spherulitic crystal. All microscopic observations were made with a polarizing microscope (POM, Olympus BX51) between crossed polars. The temperature control of a sample was performed using a hot stage (Linkam TH-600PM, Linkam Scientific Instruments, UK). The temperature of the apparatus was at 105°C. PLA resin sandwiched between microscope glass slides was heated to 200°C on a hot plate and was pressed with small stress to prepare thin film samples with desired thickness. The morphology of the thin film sample between the glass slides was observed on a hot stage and recorded on a hard disk.

Mechanical properties and HDT

The dried neat PLA and PLA/EBH blends were injection molded using an injection machine (Haitian Machinery, Ningbo, China.) operated at range of 190–195°C with the mold temperature of 30°C. The specimens were firstly annealed at 105°C for 1.0, 2.0, 5.0, 10, and 20 min. The mechanical properties of the annealed specimens were measured according to GB-T1040 method (Model 2020, Intesco, USA) with strain rate of 2 mm/min at room temperature. The HDT was measured on injection a HDT Tester (Toyoseikin Japan) according to GB-T1634 method with heating rate of 2°C/min. Notched Izod Impacts were measured according to GB-T1043.

RESULTS AND DISCUSSION

Crystallization of PLA

Crystallization rate and Crystallinity

It is very important to study the effect of EBH on crystallization rate and the crystallinity of PLA. The crystallization rate of nucleated PLA was measured by the crystallization half time obtained during

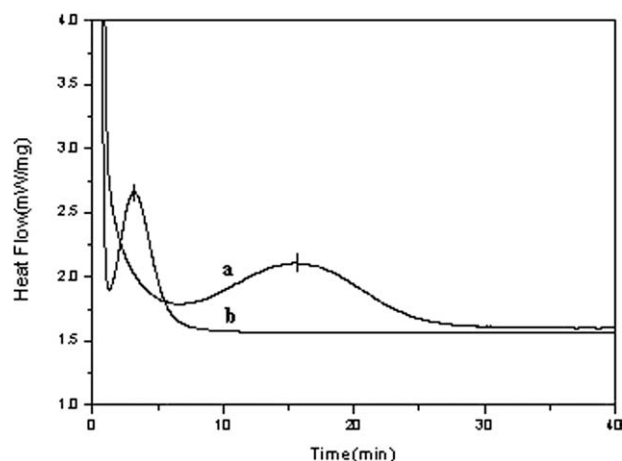


Figure 1 DSC curves of the isothermal crystallization of (a) neat PLA and (b) PLA/EBH at 105°C from the melt.

isothermal crystallization experiments.¹⁶ Using DSC, the PLA samples were heated to 200°C at a rate of 10°C/min, held for 3 min to erase thermal history, and then quickly cooled to the isocrystallization temperature of 105°C at a rate of 50°C/min, and finally held for up to 60 min. Figure 1 shows the DSC curves of neat PLA, as well as the PLA samples nucleated with 1.0% EBH. The relative crystallinity was calculated by integrating each exotherm from $t = 0$ to t and dividing by the total area under the curve. The crystallization half-time, $t_{1/2}$, was taken to be the time at which the relative crystallinity was equal to 0.5. Neat PLA had the crystallization half time of 18.8 min. The nucleated PLA containing 1.0% EBH shows crystallization half times of only 2.8 min. The nucleated PLA shows the crystallization rate by nearly sixfold over neat PLA.

The crystallinity, X_c , calculated using eq. (1) are shown in Figure 2. One hundred and five degree is

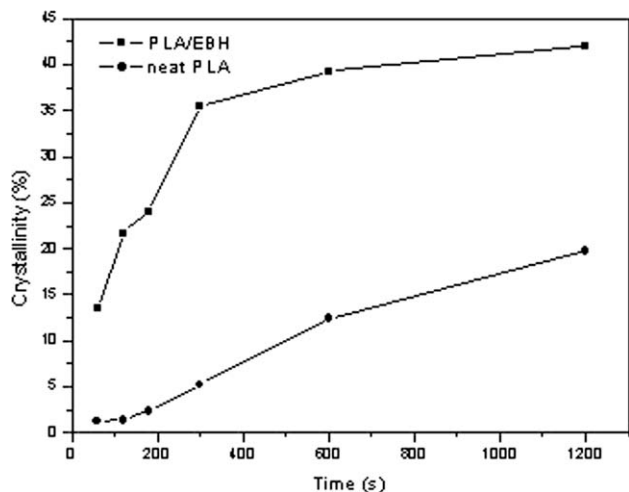


Figure 2 The curves of crystallinity for (a) neat PLA and (b) PLA/EBH at 105°C with the different annealed times.

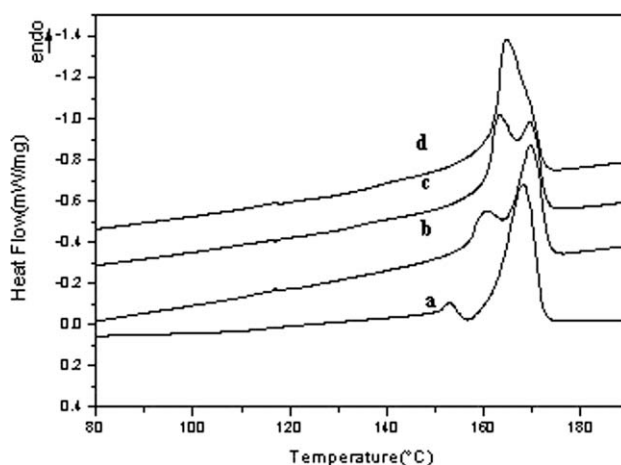


Figure 3 DSC heating curves of PLA/EBH after it was isothermally melt-crystallized for 5 min at temperatures of (a) 100°C, (b) 105°C, (c) 110°C, and (d) 115°C.

selected as crystallization temperature of PLA because the maximum crystallization temperature for PLA is between 100 and 110°C. It can be found that the X_c is about 19.0% for neat PLA at 105°C for 20 min, and the X_c increases to 42% for 20 min for the nucleated PLA at the same condition. The crystallinity of nucleated PLA would quickly increase more than 30% in 3-minute crystallization, which is much faster than neat PLA.

Isothermal crystallization

According to literature reports,^{26,29} the different crystallization temperatures affected the structural reorganization of the crystal phase of PLA that lead to multiple melting steps. Figure 3 showed the heating curves of nucleated PLA at heating rate of 10°C/min after the samples was first isothermally melt-crystallized at 100, 105, 110, and 115°C for 5 min. Double melting peaks appeared for all samples. With increasing isothermal crystallization temperature, the low endotherm (Peak L) increased in its magnitude with significant changes at the peak temperature; however, the high endotherm (Peak H) decreased in its magnitude with insignificant changes at the peak temperature. It was clear that both the shape and the position of Peak L were influenced by the crystallization temperature (T_c). The position shifted to a higher temperature range and the magnitude of the Peak L increased with the increasing crystallization temperature. For Peak H, their positions remained unchanged and their intensity decreased when the crystallization temperature was increased. According to the literatures,^{30,31} the peak temperature of the $G - T_c$ plot, where G is the spherulite growth rate, is in the range of 118–130°C for neat PLA. In this work, the T_c values studied (i.e., 100–115°C) were below this temperature

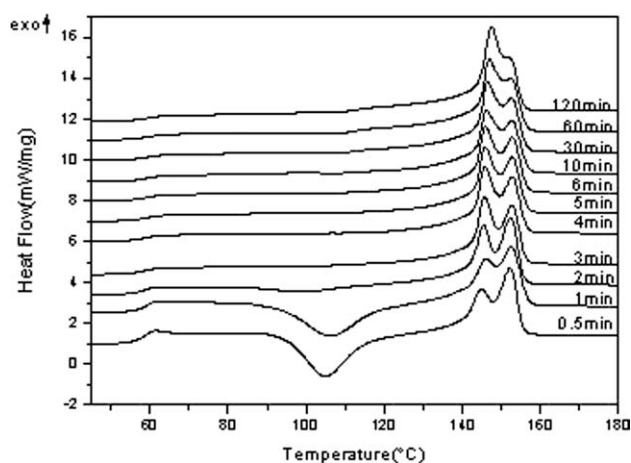


Figure 4 DSC heating curves of PLA/EBH after they were isothermally melt-crystallized at 105°C for different times of 0.5, 1.0, 2.0, 3.0, 4.0, 5.0, 6.0, 10, 30, 60, and 120 min.

range; therefore, the G values (or the crystallization rates) increased with increasing T_c in this study. A higher crystallization rate thus gave a higher peak temperature and a bigger magnitude of the low endotherm. Figure 4 showed the heating curves of nucleated PLA at heating rate of 10°C/min after the samples were isothermally melt-crystallized at 105°C for different times. As it can be seen in Figure 4, a longer crystallization time gave a bigger magnitude and higher peak temperature of the low endotherm but gave a smaller magnitude of the high endotherm with an insignificant shift at the peak temperature. Sanchez et al.³² reported that PLA exhibited a regime II to III transition temperature around 118°C based on the Lauritzen–Hoffman theory. The T_c values studied in this work are thus in regime III, in which the nucleation rate was faster than the crystal growth rate. Because the crystal growth rate in regime III can be increased with increase in T_c or time, the finding that a higher T_c or a longer time gives a bigger magnitude and a higher peak temperature of the low endotherm in Figures 3 and 4 is associated with the enhancement of the secondary crystal growth rate.²⁹

Figure 4 showed the heating curves of nucleated PLA after the samples were annealed at 105°C for 0.5, 1.0, 2.0, 3.0, 4.0, 5.0, 6.0, 10, 30, 60, and 120 min, respectively. As shown in Figure 4, double melting peaks also appeared for all samples. With increasing crystallization time at 105°C, the magnitude of the low endotherm (peak L) in the double endotherms increased and the high endotherm (peak H) decreases. The low endotherm is representative of the melting of most of the lamellae initially present. The partially melted amorphous material underwent a continuous process of recrystallization into thicker and perfect lamellae, which were melting at higher temperature.²⁹ The increase in magnitude was

accompanied by a shift at the peak position to a higher temperature. Some reports^{33,34} taught that this was caused by the fact that, at higher scanning rate, the amorphous material had less time to recrystallize. When the sample was annealed for a longer time, the lamellae thicken and became perfect.

As shown in Figures 4, it was clearly seen that the low endotherm shifted to higher temperatures and increased in magnitude with increasing annealing time at 105°C. There still existed the question of whether the crystals with the higher melting point were all formed by recrystallization during heating or whether they were, at least in part, present from the beginning of the experiment. If the high endotherm was all from the recrystallization of the melted crystals in the low melting endotherm, the magnitude of the high endotherm should not be bigger than that of the low endotherm. As it can be seen in Figure 5, the magnitude of the high endotherm in some curves was bigger than that of the low endotherm in the same curves.

To better clarify the structural reorganization of the crystal phase of PLA that leads to multiple melting peaks, the effect of heating rate was determined. Figure 5 recorded the DSC melting curves of melt-crystallized samples. The DSC curves largely changed with the heating rates and samples crystallized at 105°C. The heat flow due to the melting was small, so the DSC curves were obtained with high sensitivity. Double-melting peaks appeared in the DSC curve from heating rate = 2°C/min to heating rate = 10°C/min. As shown in Figure 5, it can be observed that Peak L increased with increasing heating rate, whereas Peak H decreased due to the various amount of high melting crystals that became perfected during the heating scans at low rates. The heating rate dependence of the peak areas of the

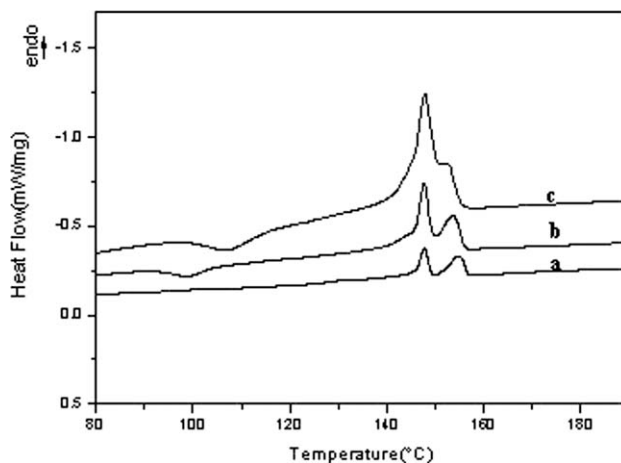


Figure 5 Melting behavior of PLA/EBH after isothermal crystallization at 105°C and heated at different heating rates of (a) 2°C/min, (b) 5°C/min, and (c) 10°C/min.

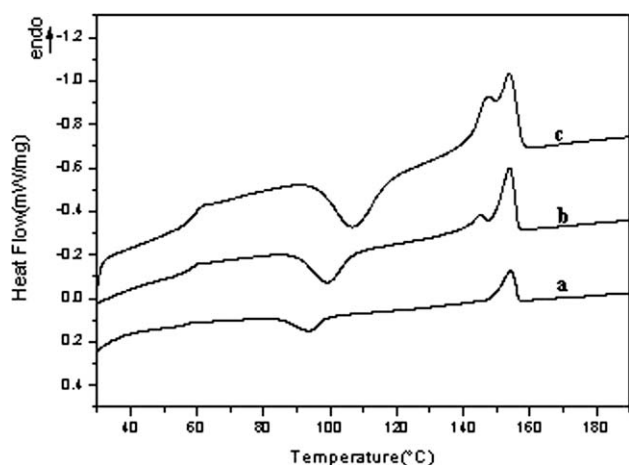


Figure 6 DSC second heating curves of PLA/EBH at different rates of (a) 2°C/min, (b) 5°C/min, and (c) 10°C/min.

double-melting peaks L and H had been reported for other semicrystalline polymers elsewhere.³⁴ The melting-recrystallization model^{35,36} suggests that small and imperfect crystals change successively into more stable crystals through the melt-recrystallization mechanism.

Nonisothermal crystallization

The nonisothermal crystallization was performed as follow: samples were first heated to 200°C at heating rate of 10°C/min, and then cooled at cooling rate of 50°C/min from the melt to 25°C, and finally recorded at certain heating rate. Figure 6 shows the second heating curves of samples at different heating rates to examine the appearance of double melting phenomena. Like neat PLA, the nucleated PLA also shows T_g at 56°C, and T_m near 154°C from Figure 6. The polymorphism behavior of PLA has been detected, which strongly relies on crystallization conditions.²⁸ As shown in Figure 6, the samples heated at 2, 5, and 10°C/min exhibit incomplete melt crystallizations, as suggested by the appearance of the exothermic peaks, respectively, during the subsequent DSC heating. The exothermic peaks that appeared during the DSC heating are attributed to cold crystallizations of PLA. This suggests that PLA exhibits slow melt-crystallization behavior. The heating rate of 2°C/min allows the smaller incomplete melt crystallization. It can be seen from Figure 6 that the double melting peaks appear in the 5 and 10°C/min heating rate cases, it can also be found that the low temperature peak height becomes higher and higher when the heating rate is higher with the heating rate of 10°C/min, whereas the higher temperature peak becomes higher and higher with the increasing of the heating rate. The height changes of the double melting peaks with increasing heating

rate indicated that the double peaks were corresponding to the melting of crystals formed during the cold crystallization and the crystallization during heating. Thus, the double melting behavior is truly due to the mechanism based on melting of the crystals formed in the cold crystallization stage during heating and followed by recrystallization and further melting processes at higher temperatures,²⁹ which is consistent with the mechanism of melt-recrystallization. It is suggested by the melt-recrystallization model that small and imperfect crystals change successively into more stable crystal through the melt-recrystallization mechanism. Because melting and recrystallization are competitive in the heating process, recrystallization is suppressed by higher heating rates.

Optical microscopy and spherulite size

The crystal growth of the nucleated PLA was observed by optical microscopy. Figure 7 shows the POM photographs of the resins crystallized at 105°C with different times. It is clearly seen that the spherulite size increases with crystallization time for neat PLA, while the spherulite size does not change much for nucleated PLA. For neat PLA, the average diameter of the spherulites was about 80 μm , and the spherulitic interface was very clear. The addition of the EBH significantly reduced the average diameter of the spherulites. And the boundaries became blurry. The small size of the spherulites would have great effect on mechanical properties, which will be discussed in Section "Mechanical properties and HDT" below.

Wide-angle X-ray scattering

First, wide-angle X-ray analyses were carried out for a series of PLA sheets that were separately annealed at 105°C for 1.0, 3.0, 10, 60, and 120 min. The results are shown in Figure 8. The WAXD patterns of those samples show only an amorphous halo when treated <3 min at 105°C. It seemed that the crystallization rate of PLA is lower outside than in DSC. Figure 4 indicated that the nucleated PLA could crystallize in half minute in DSC. The crystalline peaks start to develop when treated over 3 min and the longer the treated time, the greater the crystallinity. The WAXD results indicated that all annealed samples had the same crystalline form. This supports the argument that the double melt peaks discussed above was due to melt-recrystallization mechanism, not due to two different crystalline forms.

Figure 9 shows the WAXD results of nucleated PLA annealed at different crystallization temperatures of 80, 100, 115, and 140°C for 10 min samples, it is clearly indicated that crystallization rate is slow

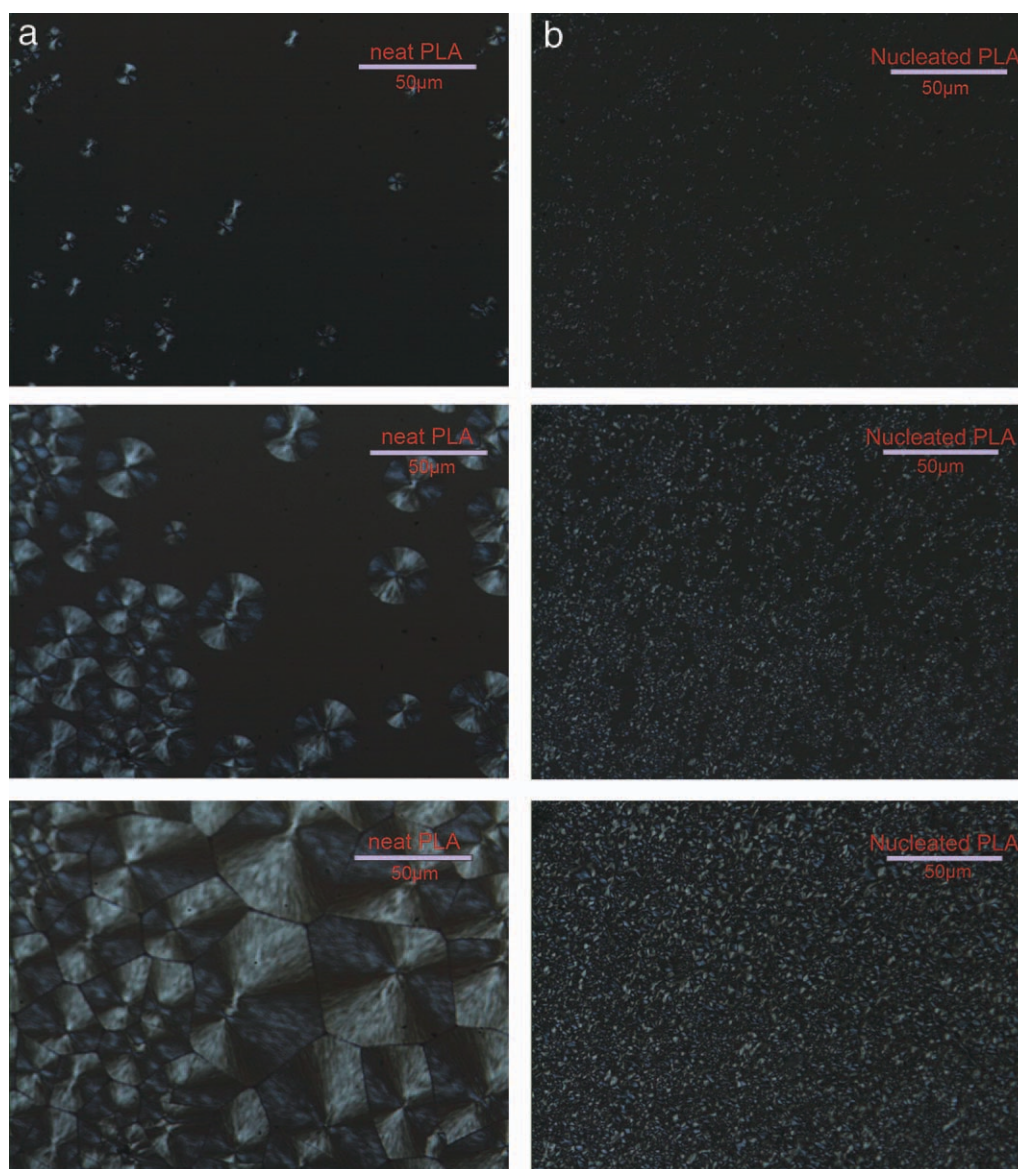


Figure 7 Optical micrographs of crystal growth at 105°C with different times: (a) neat PLA; (b) PLA/EBH. [Color figure can be viewed in the online issue, which is available at wileyonlinelibrary.com.]

at temperature below 80°C and above 130°C. At crystallization temperature of 80°C and 140°C, it is almost amorphous from WAXD patterns, which is consistent with their low crystallinity values estimated from DSC. In the range from 90 to 130°C, these results are in good agreement with crystallization kinetic data reported by other investigators.²⁸ The difference between the melt-crystallized and cold-crystallized counterpart is because of fewer nuclei existing in the melt-crystallized samples, which results in slower crystallization kinetics and, likely isolated spherulites at high temperatures. The WAXD results also indicated that the same crystalline form was obtained at different crystallization temperatures.

Mechanical properties and HDT

Notched izod impact and mechanical properties

Table I shows the impact strength of the blends. The blends enhanced the impact strength of the PLA/EBH. The impact strength of blends was higher than those of the PLA matrix itself. As shown in Table I, we can also find that the impact strength of blends improved nearly 100% from 1.4 to 2.9 KJ/m² compared to over neat PLA. This is due to reduction of spherulite size by adding the EBH showed in Figure 7. The smaller the spherulite size is, the higher the impact strength. It is consistent with the results of optical microscopy experiments. Table I also shows the Young's modulus of PLA/EBH blends with

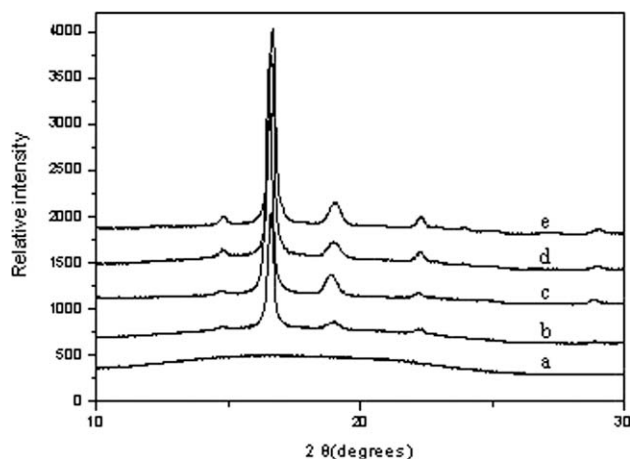


Figure 8 WAXD patterns of the PLA/EBH isothermally crystallized samples at 105°C with different annealed times of (a) 1 min, (b) 3 min, (c) 10 min, (d) 60 min, and (e) 120 min.

different annealing times. The introduction of EBH into PLA significantly improves Young's Modulus compared to the neat PLA after annealing. The modulus of nucleated PLA was increased with annealing times due to higher crystallinity obtained. It is interesting to found that both impact strength and modulus are increased with increasing crystallinity. The small crystal size of PLA leads to high impact strength.

Heat deflection temperature

The HDT of PLA/EBH blends was obtained at 0.45 MPa load with a heating rate of 2°C/min. As seen in Figure 10, the HDT of PLA/EBH blend was much higher than that of neat PLA after annealing. The HDT could be increased from 51°C of neat PLA up to 93°C of the blends. From Figures 2 and 10, it can be seen that the HDT of both neat PLA and the

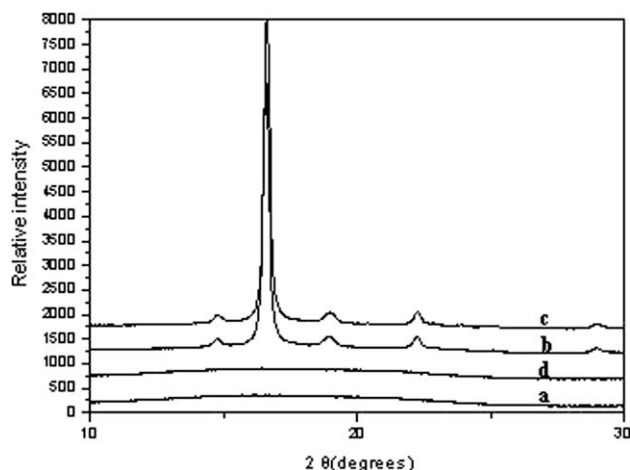


Figure 9 WAXD patterns of the PLA/EBH isothermally crystallized at different crystallization temperatures of (a) 75°C, (b) 100°C, (c) 115°C, and (d) 145°C.

TABLE I
The Physical Properties of PLA and PLA/EBH

PLA/EBH (99 : 1)	Notched Izod Impact(KJ/m ²)	Young's Modulus (MPa)
Neat PLA (Annealed 600 s)	1.4 ± 0.38	3400 ± 72
PLA/EBH (Annealed 60 s)	2.5 ± 0.08	3500 ± 62
PLA/EBH (Annealed 120 s)	2.9 ± 0.07	3500 ± 94
PLA/EBH (Annealed 300 s)	2.9 ± 0.03	3500 ± 165
PLA/EBH (Annealed 600 s)	2.5 ± 0.25	3900 ± 62
PLA/EBH (Annealed 1200 s)	2.6 ± 0.16	3900 ± 171

blend was increased with the increase of the annealed time. This improvement is mainly due to the increase of crystallinity. It is very difficult to improve HDT of PLA without increasing its crystallinity.¹⁶ According to the result shown in Figure 10, when the crystallinity exceeds 20%, the HDT starts to increase. It seems that there is a percolation threshold of crystallinity to obtain high HDT of PLA. The percolation threshold of the crystallinity is between 20 and 25% for PLA. It should be noted that neat PLA showed HDT of only 80°C at 25% crystallinity after 20-minute annealing, while nucleated PLA showed 90°C at 40% crystallinity after only 10-minute annealing (Fig. 2). This strongly indicates that it is needed to add a nucleating agent for PLA to improve HDT and molding efficiency.

CONCLUSION

The crystallization behavior and mechanical properties of nucleated PLA with EBH were thoroughly investigated. The study indicated that nucleated PLA has similar crystallization behavior to neat PLA except for high crystallization rate and small crystal size. The nucleated PLA exhibited remarkable properties on impact strength, modulus and HDT compared to neat PLA. These results were related to high crystallinity and small spherulite size of

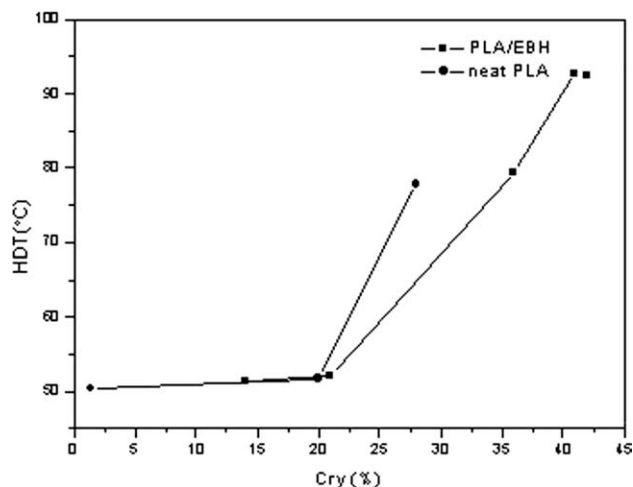


Figure 10 The curves of HDT for (a) neat PLA and (b) PLA/EBH with the different crystallinity.

nucleated PLA. The correlation between crystallinity and HDT was also established. There is a percolation threshold of crystallinity at which HDT starts to increase.

References

1. Lu, T. S.; Sun, Y. M.; Wang, C. S. *J Polym Sci Part A: Polym Chem* 1995, 33, 2.
2. Byrom, D. *Trends Biotechnol* 1987, 5, 246.
3. Martin, O.; Averous, L. *Polymer* 2001, 42, 6209.
4. Lunt, J. *Polym Degrad Stab* 1998, 59, 145.
5. Paul, M. A.; Alexandre, M.; Degée, Ph.; Henrist, C.; Rulmont, A.; Dubois, Ph. *Polymer* 2003, 44, 443.
6. Ray, S. S.; Okamoto, M. *Macromol Rapid Commun* 2003, 24, 815.
7. Solarski, S.; Ferreira, M.; Devaux, E.; Fontaine, G.; Bachelet, P.; Bourbigot, S.; Delobel, R.; Coszach, P.; Murariu, M.; Ferreira, A. D. S.; Alexandre, M.; Degee, P.; Dubois, P. *J Appl Polym Sci* 2008, 109, 841.
8. European Bioplastics. Available at: <http://www.european-bioplastics.org>.
9. Kolstad, J. J. *J Appl Polym Sci* 1996, 62, 1079.
10. Zhang, J.; Jiang, L.; Zhu, L. *Biomacromolecules* 2006, 7, 1551.
11. Pluta, M. *Polymer* 2004, 45, 8239.
12. Ray, S. S.; Yamada, K.; Okamoto, M.; Fujimoto, Y.; Ogami, A.; Ueda, K. *Polymer* 2003, 44, 6633.
13. Ray, S. S.; Yamada, K.; Okamoto, M.; Ogami, A.; Ueda, K. *Chem Mater* 2003, 15, 1456.
14. Lewitus, D.; McCarthy, S.; Ophir, A.; Kenig, S. *J Polym Environ* 2006, 14, 171.
15. Nam, J. Y.; Ray, S. S.; Okamoto, M. *Macromolecules* 2003, 36, 7126.
16. Angela, M.; Harris, Ellen, C. *J Appl Polym Sci* 2008, 107, 2246.
17. Ihn, K. J.; Yoo, E. S.; Im, S. S. *Macromolecules* 1995, 28, 2460.
18. Yoo, E. S.; Im, S. S. *J Environ Polym Degrad* 1998, 6, 223.
19. Naoshi, K.; Atsushi, S.; Takahiro, H.; Tsuyoshi, U.; Etsuo, Tobita. *J Appl Polym Sci* 2007, 103, 244.
20. Peng, S. W.; An, Y. X.; Chen, C.; F, B.; Zhuang, Y. G.; Dong, L. S. *Eur Polym J* 2003, 39, 1475.
21. Chen, C.; Bin, Fei.; Peng, S. W.; Zhuang, Y. G.; Dong, L. S.; Feng, Z. L. *Eur Polym J* 2002, 38, 163.
22. Fei, B.; Chen, C.; Wu, H.; Peng, S. W.; Wang, X. Y.; Dong, L. S.; Xin, J. H. *Polymer* 2004, 45, 6275.
23. Vasanthakumari, R.; Pennings, A. J. *Polymer* 1983, 24, 175.
24. Miyata, T.; Masuko, T. *Polymer* 1998, 39, 5515.
25. Iannace, S.; Nicolais, L. *J Appl Polym Sci* 1997, 64, 911.
26. Munehisa, Y.; Shinsuke, T.; Koji, I.; Yoshinori, O.; Yusuke, D.; Kazuhisa, T. *Polymer* 2006, 47, 7554.
27. Yasuniwa, M.; Tsubakihara, S.; Sugimoto, Y.; Nakafuku, C. *J Polym Sci Part B: Polym Phys* 2004, 42, 25.
28. Ling, X. Y.; Joseph, E. *J Polym Sci Part B: Polym Phys* 2006, 44, 3378.
29. Shieh, Y. T.; Liu, G. L. *J Polym Sci Part B: Polym Phys* 2007, 45, 466.
30. Di Lorenzo, M. L. *Polymer* 2001, 42, 9441.
31. Krikorian, V.; Pochan, D. J. *Macromolecules* 2004, 37, 6480.
32. Sanchez, M. S.; Ribelles, J. L. G.; Sanchez, F. H.; Mano, J. F. *Thermochim Acta* 2005, 430, 201.
33. Maria, L.; Di, L. *J Appl Polym Sci* 2006, 100, 3145.
34. Yasuniwa, M.; Satou, T. *J Polym Sci Part B: Polym Phys* 2002, 40, 2411.
35. Wunderlich, B. *Macromolecular Physics*; Academic press: New York, 1980; Vol.3.
36. Yasuniwa, M.; Tsubakihara, S.; Ohoshita, K.; Tokudome, S. *J Polym Sci Part B: Polym Phys* 2001, 39, 2005.